

On the composition dependence of the microscopic structure, thermodynamic, dynamic and dielectric properties of water-dimethyl formamide model mixtures. Molecular dynamics simulation results

H. Dominguez, O. Pizio*

Instituto de Investigaciones en Materiales, Universidad Nacional Autónoma de México, Circuito Exterior, 04510, México, D.F., México

Received August 10, 2017, in final form September 11, 2017

Isothermal-isobaric molecular dynamics simulations have been performed to examine an ample set of properties of the model water-N,N-dimethylformamide (DMF) mixture as a function of composition. The SPC-E and TIP4P-Ew water models together with two united atom models for DMF [Chalaris M., Samios J., J. Chem. Phys., 2000, **112**, 8581; Cordeiro J., Int. J. Quantum Chem., 1997, **65**, 709] were used. Our principal analyses concern the behaviour of structural properties in terms of radial distribution functions, and the number of hydrogen bonds between molecules of different species as well as thermodynamic properties. Namely, we explore the density, excess mixing molar volume and enthalpy, the heat capacity and excess mixing heat capacity. Finally, the self-diffusion coefficients of species and the dielectric constant of the system are discussed. In addition, surface tension of water-DMF mixtures has been calculated and analyzed.

Key words: *water models, N,N-dimethylformamide models, thermodynamic properties, self-diffusion coefficient, dielectric constant, surface tension, molecular dynamics*

PACS: 61.20.-p, 61.20-Gy, 61.20.Ja, 65.20.Jk

1. Introduction

N,N-dimethylformamide (DMF) is a multipurpose organic solvent with widespread applications in chemistry and related areas of much practical importance, see e.g., [1–3]. In several processes it is used as a co-solvent. On the other hand, as one example of amides, it is frequently chosen as a model system for peptides. Given the importance of DMF and of its mixtures with water and several organic solvents, investigation of the properties of such complex molecular systems has been undertaken using a variety of experimental techniques. Namely, the studies of microscopic structure have been performed using neutron and electron diffraction, NMR and dielectric spectroscopy; data resulting from measurements of various properties, like density, excess molar volume and enthalpy, excess molar heat capacity, self-diffusion coefficients, dielectric constant have been reported in [4–25]. Some experimental observations were supported by quantum chemical calculations [26, 27].

In addition, aiming at rather general and more profound insights into the behavior of various properties on temperature, pressure and chemical composition of water-DMF mixtures and at interpretation of experimental data, computer simulation methods have been applied to these mixtures. N,N-dimethylformamide is an interesting molecule, hydrophobic methyl groups can disturb the water structure. Besides, “cross” hydrogen bonds are expected to form between molecules belonging to two different species. Computer modelling studies can be classified according to the details of the force fields describing the internal structure of the DMF molecule. Specifically, one set of models with either five or six force centers (in

*On sabbatical leave from Instituto de Química de la UNAM, corresponding author: oapizio@gmail.com.

each of models the methyl group has been considered as a single site) was explored in [28–39]. Another set of apparently more sophisticated models, i.e., at all-atom level, has been designed and then studied in detail in several publications [40–44]. A very comprehensive description of the properties of an ample set of organic liquids resulting from simulations with various force fields has been discussed in [45] (see also the file that contains a vast supporting information of [45] and the <http://virtualchemistry.org> web site).

In this work we restrict our attention solely to the modelling of water-DMF mixtures and to the critical evaluation of several properties as a function of composition resulting from isobaric-isothermal computer simulations. Moreover, our attention is restricted to the united-atom type models for DMF molecule developed by Cordeiro and by Chalaris and Samios. The reason of studying these models, in addition to and in spite of the available knowledge, is that we believe several even basic issues have not been comprehensively and critically discussed. Specifically, we calculate density and excess mixing density, excess mixing volume and enthalpy, heat capacity and excess mixing heat capacity, self-diffusion coefficients of species of the mixture, dielectric constant and the excess dielectric constant, average number of hydrogen bonds, all as functions of mixture composition. The microscopic structure is briefly discussed in terms of the pair distribution functions. Finally, we performed calculations of the surface tension switching to the constant volume-constant temperature canonical ensemble. For the majority of properties calculated, we perform comparisons with the experimental results. Having in mind our recent investigation of the properties of water-methanol [46, 47], water-DMSO [48] and water-1,2-dimethoxyethane (DME) mixtures [49], the results of the present work are discussed in a wider context in qualitative terms, making comparisons of the trends observed for different organic liquids mixed with water.

Exploration of the behavior of water-DMF mixtures by using all-atom type models for DMF will be presented elsewhere in a separate work. Our longer term objective of the project, however, is in the theoretical exploration of the behavior of solutes of different complexity in water-DMF and other water-organic liquid mixtures in the spirit of important and interesting experimental studies [50–53].

2. Models and simulation details

Our calculations have been performed in the isothermal-isobaric (NPT) ensemble (at 1 bar, and at a temperature of 298.15 K), unless specified in the surface tension subsection. We used the GROMACS package [54] version 4.6.5. For water in the present study, the SPC-E model [55] and the TIP4P-Ew model [56] were used. As for the DMF molecules, we explore two united-atom type models with six force sites, H, O, C, N, each methyl group, CH₃ is considered as a single site, C3. The nomenclature of the DMF models is as follows: we use the model and notation CS2 as proposed by Chalaris and Samios, see table I of [34]. On the other hand, the model denominated as Cordeiro is the one proposed by this author and described in detail in table I of [30]. All the parameters for the intramolecular geometry of the rigid CS2 model are given in table II of [34]. The model of Cordeiro is rigid as well. For the sake of numerical convenience, in the present work we relaxed rigidity of bonds and angles, taking the force constants from the OPLS data basis as appropriate. Moreover, to keep the DMF molecule planar, the improper dihedral angle for H-C-N-C3 and for O-C-N-C3 has been assumed from the OPLS data basis as well.

The geometric combination rule (rule 3 in GROMACS nomenclature) has been applied for cross interactions in all our calculations. The nonbonded interactions were cut off at 1.4 nm, and the long-range electrostatic interactions were handled by the particle mesh Ewald method implemented in the GROMACS software package (fourth order, Fourier spacing equal to 0.12). The van der Waals tail correction terms to the energy and pressure were taken into account. In order to maintain the geometry of water and DMF molecules, LINCS algorithm was used.

For each system a periodic cubic simulation box was set up. The GROMACS genbox tool was employed to randomly place all particles into the simulation box. The total number of molecules was kept fixed at 3000. The composition of the mixture is described by the mole fraction of DMF molecules, X_{dmf} , $X_{\text{dmf}} = N_{\text{dmf}} / (N_{\text{dmf}} + N_{\text{w}})$.

To remove possible overlaps of particles introduced by the procedure of preparation of the initial configuration, each system underwent energy minimization using the steepest descent algorithm imple-

mented in the GROMACS package. Minimization was followed by a 50 ps NPT equilibration run at 298.15 K and 1 bar using a timestep of 0.25 fs. We applied the Berendsen thermostat and barostat with $\tau_T = 1$ ps and $\tau_P = 1$ ps during equilibration. Constant value of $4.5 \times 10^{-5} \text{ bar}^{-1}$ for the compressibility of the mixtures was set up. The V-rescale thermostat and Parrinello-Rahman barostat with $\tau_T = 0.5$ ps and $\tau_P = 2.0$ ps and the time step 2 fs were used during all production runs. To test the thermostat and barostat, we have obtained 88.5 J/mol·K for the heat capacity of the SPC/E model, this value being close to 86.6 J/mol·K reported by Vega et al. [57] (experimental result is 75.3 J/mol·K). On the other hand, we obtained 155.55 J/mol·K for the heat capacity of the DMF for the CS2 model, and 158.78 J/mol·K for the Cordeiro model, the experimental values reported from independent measurements are as follows: 150.16 J/mol·K [14], 150.8 J/mol·K [11]. Moreover, the DMF molar volume coming out from our calculations is 76.53 cm³/mol (CS2 model) and 78.23 cm³/mol (Cordeiro model), the deviation from the experimental result, 77 cm³/mol, is very small in the case of CS2. Berendsen type control of temperature and pressure is not satisfactory in this aspect.

Statistics for each mole fraction for some of the properties were collected over several 10 ns NPT runs, each started from the last configuration of the preceding run. The total trajectory was not shorter than 60 ns. Actually, the heat capacity and the dielectric constant are the most time demanding properties.

3. Results and discussion

3.1. Density, mixing properties

We begin a discussion of the results by presenting the dependence of density of water-DMF mixture with united-atom type models for DMF on composition, panel (a) of figure 1. In spite of a meticulous search, we have not found previous comparisons of this sort. Two water models and two DMF models are involved. The experimental data are taken from [10, 11]. Experimental results show a peculiar behavior of mixture density at low values of X_{dmf} , namely while DMF is added to water, the mixture density exhibits a weakly pronounced maximum, at $X_{\text{dmf}} < 0.2$, the density preserves values close to the density of pure water, if X_{dmf} is low. Actually, $\rho(X_{\text{dmf}})$ decreases with DMF concentration only for $X_{\text{dmf}} > 0.2$. A combination of SPC-E and Cordeiro model leads to a pronounced underestimation of density in the entire composition range. On the other hand, the SPC-E-CS2 as well as TIP4P-Ew-CS2 exhibit a more satisfactory behavior. Both models underestimate the values of density of the mixture at small values of X_{dmf} and slightly overestimate the density for high values of X_{dmf} .

It is common to characterize the behavior of various properties of binary mixtures in terms of excess

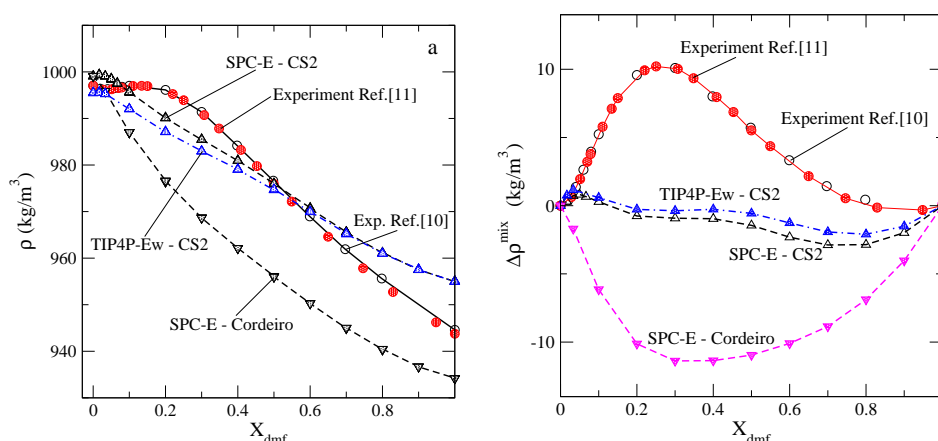


Figure 1. (Color online) Panel (a): Composition dependence of the density of water-DMF mixtures from constant pressure-constant temperature simulations ($T = 298.15$ K, $P = 1$ bar) in comparison with the experimental data from [10, 11]. Panel (b): Excess mixing density on composition.

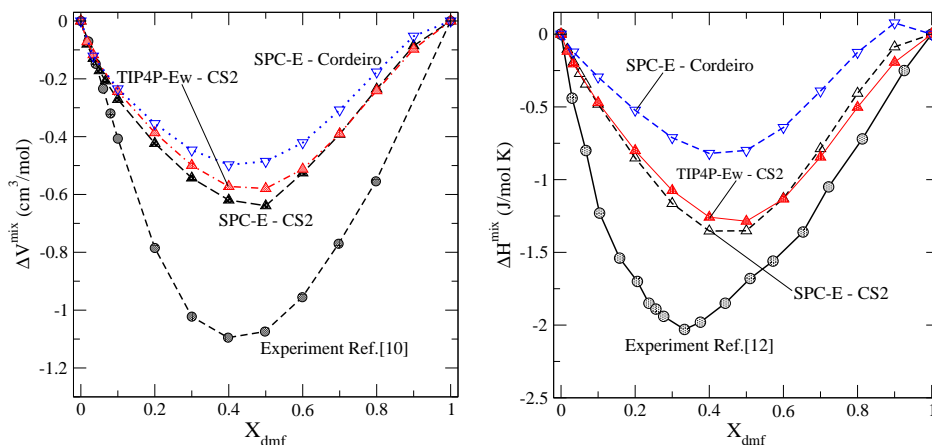


Figure 2. (Color online) Excess mixing molar volume and excess mixing enthalpy of water-DMF mixtures on composition.

mixing contribution as follows,

$$\Delta Y^{\text{mix}} = Y_{\text{m}} - [X_1 Y_1 + (1 - X_1) Y_2], \quad (1)$$

where Y_{m} refers to the mixture at a given composition, Y_i ($i = 1, 2$) are the values for pure components, Y can be any property of the mixture, e.g., density or volume or enthalpy or another one.

Here, to begin with, we obtain a finer insight into the decay of density from pure water to pure DMF. It is provided by the results given in panel (b) of figure 1. Namely, the deviation of mixture density from an ideal type behavior is closer to the experimental trends if the SPC-E or TIP4P-Ew water models are combined with the CS2 model for DMF. On the other hand, predictions of the SPC-E combined with Cordeiro model are not satisfactory. Positive deviation of excess mixing density is similar to what was observed in mixtures of alcohols with water in the work of Wensink [58]. In fact, the behavior of excess mixing density can indicate the accuracy of theoretical curves, but it does not provide explicit insights into the mixing trends; methanol or ethanol mix with water perfectly well, but the $\Delta\rho$ is positive in the entire range of composition.

The excess mixing volume and enthalpy are given in two panels of figure 2. From panel (a) of this figure we learn that the excess mixing volume describes a contraction of the mixture upon composition qualitatively well, although the magnitude of ΔV^{mix} is underestimated. The minimum value from the simulations is at $X_{\text{dmf}} \approx 0.5$, whereas the experimental result attains minimum at $X_{\text{dmf}} = 0.4$. The closest, to the experiment, set of theoretical data comes out from the SPC-E-CS2 model.

One can see quite similar trends in the behavior of excess mixing enthalpy, panel (b) of figure 2. The values for $\Delta H^{\text{mix}}(X_{\text{dmf}})$ are underestimated by all the models considered and the minimum occurs at a slightly higher X_{dmf} (between 0.4 and 0.5), in comparison to the experimental result at $X_{\text{dmf}} \approx 0.35$. Again, the SPC-E-CS2 model is better comparing to, e.g., SPC-E-Cordeiro version of the model. In general, one can conclude that the united-atom type models of this work underestimate geometric and energetic trends for mixing of species given by ΔV^{mix} and by ΔH^{mix} in the entire interval of mixture compositions. The agreement with the experimental results is qualitative for both properties in question.

In addition, it is worth studying the energetic trends of mixing of species in terms of fluctuations. Namely, in figure 3 we explore the dependence of the constant pressure heat capacity and the corresponding excess property as functions of mixture composition. Actually, the situation is rather satisfactory. From panel (a) of figure 3, we learn that trends of dependence of C_P on X_{dmf} are well reproduced by all the models studied, just the theoretical curves are shifted upward in comparison to the experimental dependence. The shape and magnitude of ΔC_P^{mix} is reproduced by the simulated models very well. Moreover, the maximum is predicted at 0.4 whereas in the experiment it is at ≈ 0.3 . Seemingly, the SPC-E-CS2 combination of models is the best in this aspect.

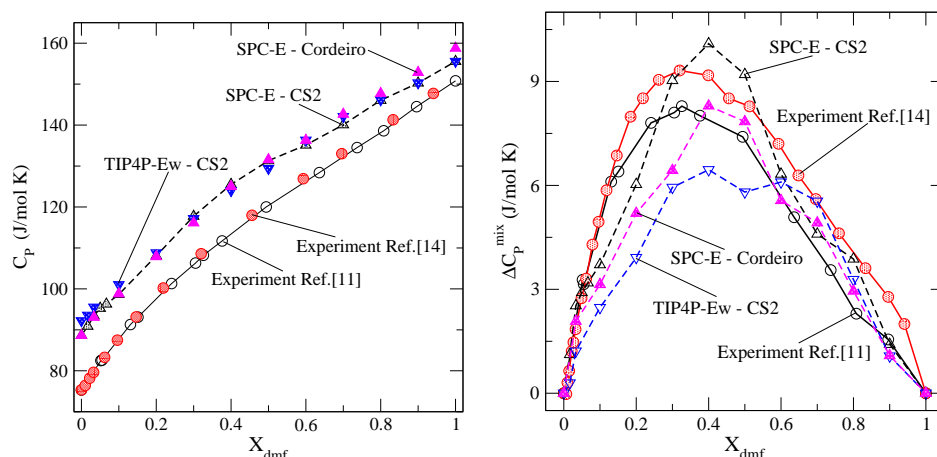


Figure 3. (Color online) Panel (a): Composition dependence of the heat capacity at constant pressure of water-DMF mixtures from constant pressure-constant temperature simulations ($T = 298.15$ K, $P = 1$ bar) in comparison with the experimental data from [11, 14]. Panel (b): Excess mixing constant pressure heat capacity on composition in comparison with experimental data.

After exploring thermodynamic aspects of mixing, we proceed to the brief description of the microscopic structure in terms of the pair distribution functions and hydrogen bonding between molecules.

3.2. Pair distribution functions, hydrogen bonding

All the pair distribution functions discussed below result from simulations of the SPC-E-CS2 model. We have checked, however, that other models, like TIP4P-Ew-CS2 and SPC-E-Cordeiro, yield a qualitatively similar picture of the trends observed.

The system is characterized by a large set of the site-site distribution functions. Our focus is only in some of them, namely in the functions that describe most essential changes of the structure of the system upon changes of its chemical composition. Evolution of the distribution of DMF molecules on changes of X_{dmf} is shown in terms of the distribution functions between DMF oxygens, OD-OD (notation OD is used as an abbreviation for O_{dmf}), see two panels of figure 4. If the DMF molecules are at small amount in the medium with predominant number of waters, the DMF particles seem preferring to stay rather close

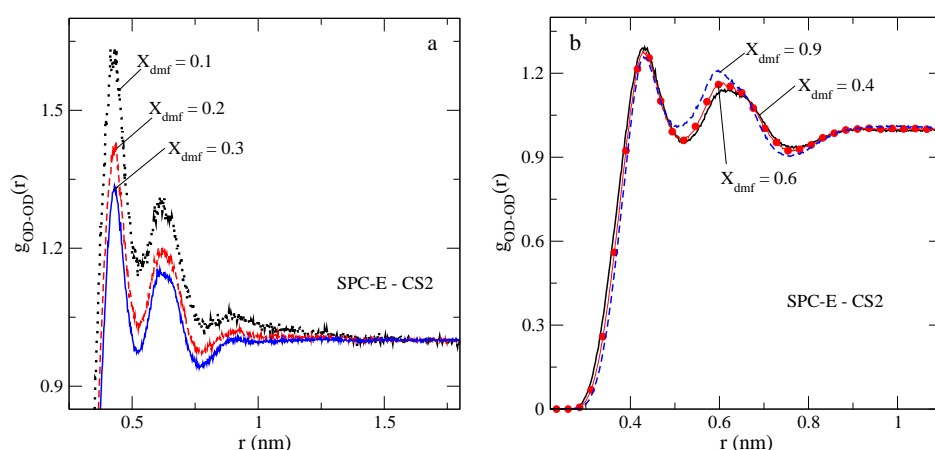


Figure 4. (Color online) Evolution of the pair distribution functions, OD-OD, with changing solvent composition.

to one another, as it follows from the first two maxima of the pair distribution function (pdf) in panel (a) of figure 4. However, even the first maximum is not high, the second one is much lower, hence mutual contacts of two and more DMF molecules are not very probable. If the concentration of DMF species increases, their distribution becomes even more “homogeneous”, see, e.g., the curves are $X_{\text{dmf}} = 0.2$ and 0.3 in panel (a). In other words, the first and second maxima as well as the minimum between them, all slightly decrease in magnitude and at larger inter-particle separations, the pdf is close to unity. This rather uniform distribution of DMF species, does not change significantly in an ample interval of compositions, say from $X_{\text{dmf}} = 0.3$ up to $X_{\text{dmf}} = 0.9$. Moreover, we do not observe a shift of the position of the first maximum of the pdf. It is located at $r \approx 0.43$ nm. Only, the second maximum of the OD-OD distribution slightly grows and shifts to smaller inter-particle separations when the composition changes from $X_{\text{dmf}} = 0.4$ up to $X_{\text{dmf}} = 0.9$, indicating a weakly enhanced “crowding” of the DMF particles if their amount increases. At this point we would like to refer to the visualization of the distribution of a small amount of DMF molecules in the “sea” of waters, see figure 5, panel (a). This snapshot corresponds to the final configuration of particles after ≈ 60 ns. Both, the pdf at a low value of X_{dmf} and the snapshot at similar conditions, permit to conclude that there is no clustering of DMF species.

Let us proceed now to the description of the evolution of distribution of water molecules in terms of the pdf OW-OW, figure 6. The most pronounced trend is that the first maximum of $g_{\text{OW-OW}}$ strongly increases in magnitude upon increasing X_{dmf} , i.e., when the concentration of water species decreases. However, important observation is that such a behavior is not accompanied by a substantial growth of the second maximum of this function. To summarize, the contacts between water molecules become more and more probable whereas the probabilistic aspects of the structure of organic subsystem are less affected by changes of X_{dmf} . Water molecules efficiently fill the space between the DMF particles, cf. the OW-OW first maximum grows at $r \approx 0.28$ nm whereas the OD-OD first maximum remains almost intact at $r \approx 0.43$ nm. The shape of OW-OW pdf together with the typical configuration of molecules given in the snapshot, right-hand panel of figure 5, leads to the conclusion that water molecules are rather uniformly distributed in the “sea” of DMF particles, closely situated waters are restricted to pairs at most.

Next, we would like to explore the trends of cross correlations between particles belonging to different species in this binary mixture. We analyze them by using the OW-OD and OD-HW distribution functions. A few representative examples are shown in figure 7. The shape of the pdf OW-OD changes principally at small interparticle separations. Namely, the first maximum increases in magnitude with an increasing X_{dmf} in the entire range of composition, starting from low values of X_{dmf} up to the high values. Its position on the r -axis does not change, however. As we have seen from figure 4, the shape of OD-OD is

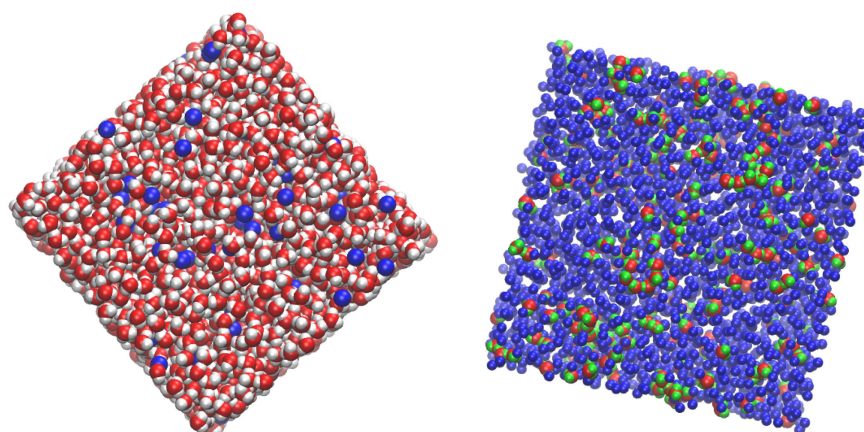


Figure 5. (Color online) Visualization of the distribution of DMF molecules (nitrogen atoms — blue spheres) in water medium ($X_{\text{dmf}} = 0.03333$) in the left-hand panel (water oxygens and hydrogens — red and grey spheres, respectively), and of the distribution of water molecules in the DMF medium (nitrogens — blue spheres) at $X_{\text{dmf}} = 0.9$ in the right-hand panel (water oxygens and hydrogens — red and green spheres, respectively).

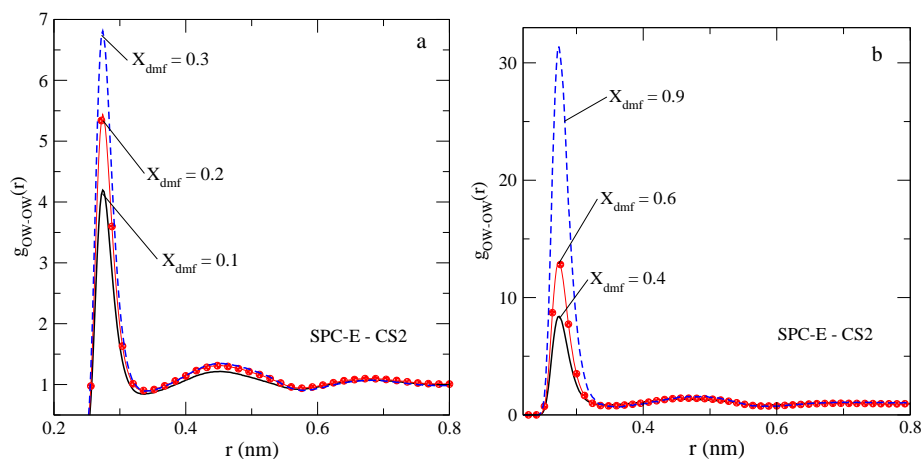


Figure 6. (Color online) Evolution of the pair distribution functions, OW-OW, with changing solvent composition.

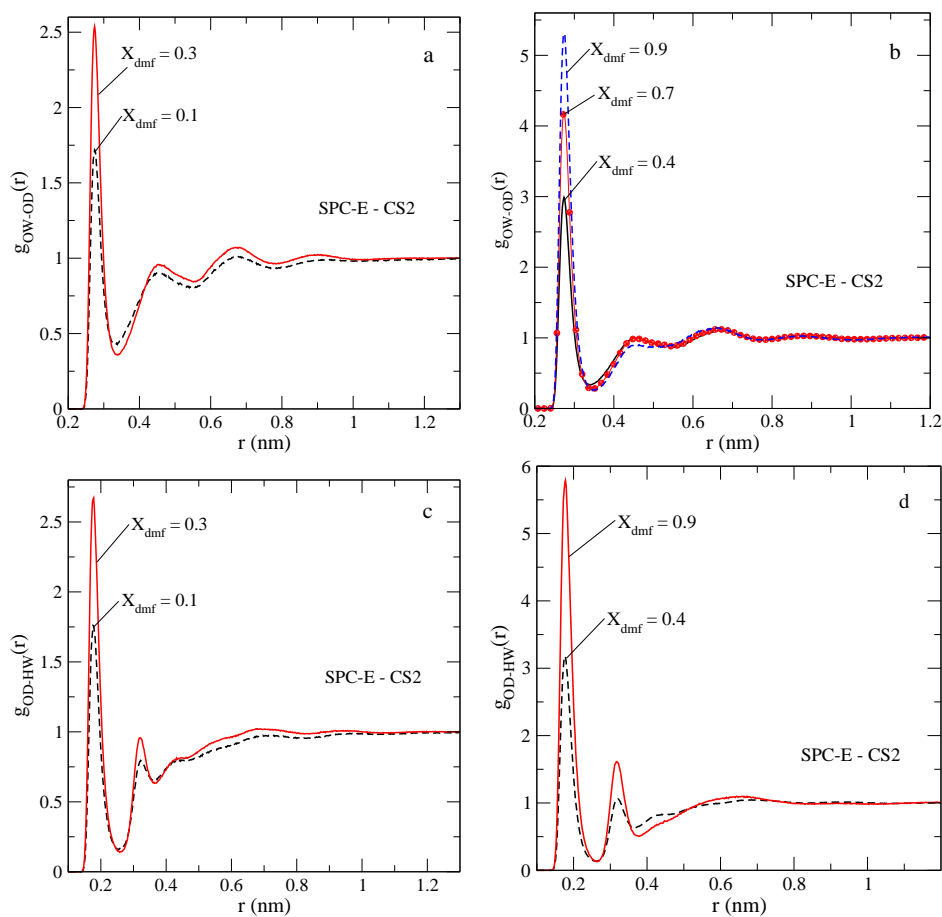


Figure 7. (Color online) Evolution of the pair distribution functions, OW-OD, and OD-HW with changing solvent composition.

weakly affected by X_{dmf} values, thus changes of the function OW-OD are quite small in the interval from $r \approx 0.4$ nm up to $r \approx 1$ nm. In contrast to this behavior, the function OD-HW is sensitive to the value of X_{dmf} in the region of the first and of the second maximum. The first maximum of the OD-HW pdf

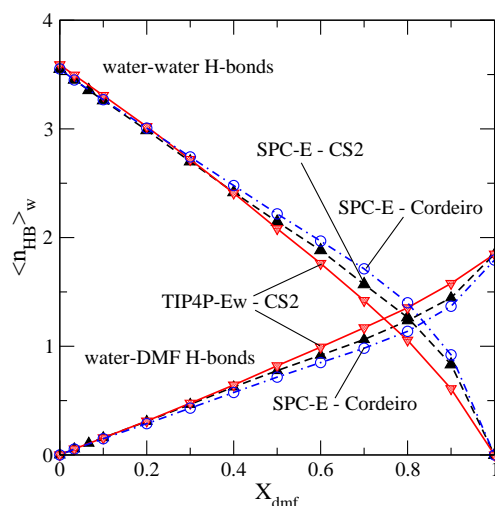


Figure 8. (Color online) Changes of the average number of water-water and water-DMF hydrogen bonds (per water molecule) upon composition changes. The cross water-DMF bonds for SPC-E-CS2 model are given by solid black triangles up.

substantially increases in magnitude with an increasing X_{dmf} . Concerning the second maximum of this function, it can be seen that its growth can be related to changes of the OW-OW pdf. Namely, the second maximum of OD-HW becomes higher than unity for $X_{dmf} > 0.4$. Development of this maximum can be attributed to an essential growth of OW-OW first maximum at a high concentration of DMF molecules in the mixture. It is intuitively expected that hydrogen bonded water molecules occupying the space close to OD atom predominantly contribute to this second maximum of OD-HW, because if hydrogens belonging to two different water molecules are close to OD, they should contribute to the first maximum.

Our final concern in this subsection is in the trends of behavior of the average number of hydrogen bonds (normalization is performed per water molecule) between water molecules as well as cross water-DMF bonds (figure 8). The GROMACS software using a default distance-angle criterion was applied to count the numbers of bonded molecules in each case. The behavior of $\langle n_{HB} \rangle$ as a function of X_{dmf} is qualitatively similar to what was recently discussed for other water-organic liquid mixtures [48, 49]. The average number of H-bonds between water molecules decreases whereas the fraction of the bonds between water molecules and DMF oxygen steadily increases with an increasing fraction of DMF species. Only at very low values of X_{dmf} , the value for water-water $\langle n_{HB} \rangle$ is high, yielding evidence of the hydrogen bonded network between water molecules. If DMF species are introduced into water, the number of cross contacts increases, as it follows from the OW-OD and OD-HW functions, cf. panels (a) and (d) of figure 7. At high values of X_{dmf} , the average value of cross bonds becomes higher than the one between waters. This is explicable straightforwardly, because at high concentration of DMF species in the mixture there is no room to form fragments of expanded network of hydrogen bonds and, besides, the majority of water molecules are surrounded by DMF, either as individual entities or very small groups such as pairs. It is difficult to establish precisely at what values of X_{dmf} the hydrogen bonded network cease to exist as such. That would require additional and a more profound analysis of a set of topologic elements characterizing the cooperativity of bonds. All three models explored in the present work (SPC-E-CS2, TIP4P-Ew-CS2 and SPC-E-Cordeiro), provide a qualitatively similar picture concerning $\langle n_{HB} \rangle(X_{dmf})$. Fine details depend on water modelling and on the internal structure of DMF molecule. A model that predicts slightly more probable water-water bonding in consequence leads to a slightly smaller fraction of water-DMF bonds. For the moment, we have not explored the life-time and strength of the bonds formed in the system, however.

Nevertheless, one more remark is pertinent. As we have seen above, maxima on the experimentally measured excess mixing properties are observed in the interval $0.3 < X_{dmf} < 0.4$ (cf. figures 2 and 3) whereas the simulation predictions for the extrema are in the interval $0.4 < X_{dmf} < 0.5$. This interval

of compositions seems to correspond to the systems in which the effect of hydrogen bonded network gradually ceases. It is tempting to attribute this change of the behavior to the range of compositions in which the curves for $\langle n_{\text{HB}} \rangle(X_{\text{dmf}})$ start to deviate from linearity. However, this hypothesis should be explored and possibly confirmed by more sophisticated tools. Now, we would like to see if these observations of the trends of thermodynamic and structural properties are related to dynamic properties.

3.3. Self-diffusion coefficients

One of the principal objectives of the present study is to combine a discussion of an ample set of properties of water-DMF mixtures. Their dynamic properties undoubtedly deserve a separate work. Here, we focus solely on the self-diffusion coefficients of water and DMF species. As usual, they are calculated from the mean-square displacement (MSD) of a particle via Einstein relation,

$$D_i = \frac{1}{6} \lim_{t \rightarrow \infty} \frac{d}{dt} \langle |\mathbf{r}_i(\tau + t) - \mathbf{r}_i(\tau)|^2 \rangle, \quad (2)$$

where i refers to water or DMF molecules and τ is the time origin. Default settings of GROMACS were used for the separation of the time origins. A set on trajectories coming from several consecutive simulations of 10 ns were combined to get an entire trajectory not less than 60–70 ns. The fitting interval then has been chosen from $\approx 10\%$ to $\approx 50\%$ of the entire trajectory, to obtain D_{dmf} and D_{w} . A set of results coming from the application of three models is given in two panels of figure 9. In spite of an extensive search in the literature, we have found only one set of experimental data describing D_{dmf} self-diffusion coefficient at $T = 293$ K. Our calculations refer to $T = 298.15$ K, however. An overall shape of $D_{\text{dmf}}(X_{\text{dmf}})$ is similar from experiments and from simulations of the models, panel (a) of figure 9. At each end of the curves there is a maximum value separated by a minimum, the minimum in experiment is at $X_{\text{dmf}} \approx 0.2$ whereas all the simulated models predict a minimum at ≈ 0.3 . Moreover, the models used in simulations yield lower values for D_{dmf} in a wide interval of compositions, from 0.1 to 1, comparing to experimental data. Only at a rather low X_{dmf} , less than 0.1, the simulations predict higher values for D_{dmf} than from experiment.

The self-diffusion coefficient of water species in binary water-DMF mixtures is presented in panel (b) of figure 9. Unfortunately, we were unable to find the experimental data in spite of the efforts. One well documented point is for pure water [57]. Starting from this point, the values for D_{w} substantially decrease with an increasing X_{dmf} till the minimum at $X_{\text{dmf}} = 0.5$. The value of D_{w} at minimum is approximately five times lower than for pure water. While X_{dmf} increases further, the self-diffusion coefficient, D_{w} , increases in magnitude to reach the values above unity (twice higher value than at minimum) for mixtures

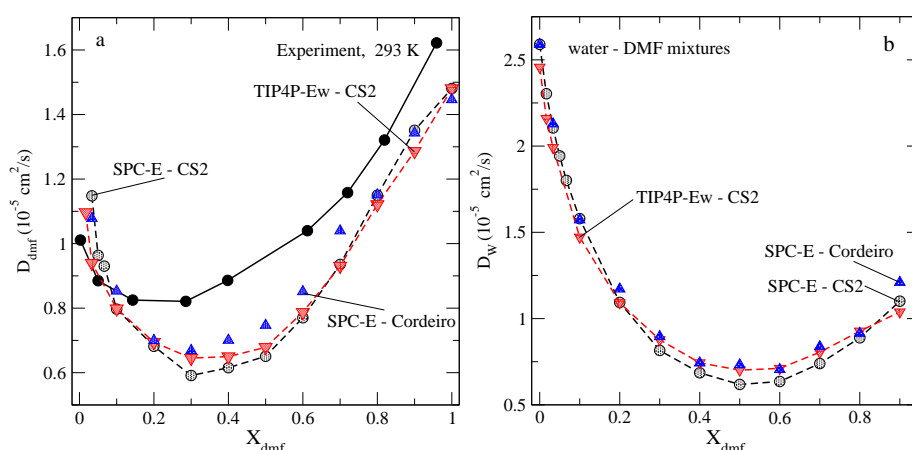


Figure 9. (Color online) Composition dependence of the self-diffusion coefficients of species in water-DMF mixtures from constant pressure-constant temperature simulations ($T = 298.15$ K, $P = 1$ bar). In panel (a) the experimental data are taken from [9] at $T = 293$ K.

predominantly composed of DMF species. Thus, for water-rich mixtures, D_w is much higher than D_{dmf} , in contrast to DMF-rich mixtures, where D_{dmf} is higher than D_w . Note that the y -scale is different in two panels. The magnitudes of D_{dmf} and of D_w at respective minima are close to each other.

Huge difference between the self-diffusion coefficients of each species at two opposite sides of the composition axis leads to the conclusion that there exists only a weak coupling of the dynamics of water and DMF particles. At low X_{dmf} , the self-diffusion coefficient of water D_w is approximately twice higher than D_{dmf} . One can suppose that a molecule of DMF is trapped in a water medium. The existence of the hydrogen bond network does not suppress the self-diffusion of water molecules but contributes to diminish self-diffusion of an individual DMF molecule in such a surrounding. On the other hand, on the opposite side, for DMF-rich mixtures, the self-diffusion of a water molecule is suppressed much less comparing to DMF, cf. ratio of D_{dmf} and of D_w at high X_{dmf} . The strongest coupling of the dynamics of two species is observed at intermediate values of composition ($0.3 < X_{\text{dmf}} < 0.5$), i.e., in the interval where the deviations from ideality of thermodynamic characteristics are at maximum. At these composition values, it seems that the effects of a hydrogen bonding between particles become much less important since the network cease to exist as such, and just the packing and energetic aspects of mixing for systems close to equimolarity determine the minima of the self-diffusion coefficients. It would be of interest to extend the exploration of the dynamic properties by calculating viscosity and characteristic relaxation times for mixtures of different composition. A broader set of properties — stronger conclusions should come out.

3.4. Composition dependence of the dielectric constant

Finally, we would like to put attention at one of various manifestations of the dielectric properties. The long-range, asymptotic behavior of correlations between molecules possessing, e.g., a dipole moment is determined by the dielectric constant, ϵ . It is commonly accepted that long molecular dynamics runs are necessary to obtain reasonable estimates for this property, because ϵ is calculated from the time-average of the fluctuations of the total dipole moment of the system,

$$\epsilon = 1 + \frac{4\pi}{3k_BTV} (\langle \mathbf{M}^2 \rangle - \langle \mathbf{M} \rangle^2), \quad (3)$$

where k_B is the Boltzmann constant and V is the simulation cell volume. In this work we have taken care that each of the runs is of sufficient length, not less than 60 ns in the majority of cases. The curves coming out from simulations for three models of water-DMF mixtures are shown in figure 10 (a). A general trend of the behaviour of $\epsilon(X_{\text{dmf}})$ is that it decreases with an increasing X_{dmf} , starting from a high value for pure water to a lower value corresponding to pure DMF. As it follows from the comparison of the simulation results and experimental data [13], all three models substantially underestimate the values for ϵ in the entire composition range. The static dielectric constant for pure DMF in the framework of CS2 model is $\epsilon \approx 27.83$, whereas for the model of Cordeiro it is 28.52, the experiment yields 39.88 [13]. On the water-rich side, the discrepancy between simulation data and experimental value evidently results from water modelling. It is highly probable to improve the dependence of the static dielectric constant on composition by applying the model for water specifically parametrized to reproduce the dielectric constant [59]. Simultaneously, it would require parametrization of the force field for the DMF molecule. This task seems to be attainable.

Another sensitive test is provided by a comparison of the excess dielectric constant [see equation (1)], $\Delta\epsilon^{\text{mix}} = \epsilon_m - [X_{\text{dmf}}\epsilon_{\text{dmf}} + (1 - X_{\text{dmf}})\epsilon_w]$, with the experimental predictions [13]. Experimental points indicate a negative deviation from ideality in the entire composition range, figure 10 (b). Interestingly, this behaviour is contrary to what follows for water-DMSO liquid mixtures [48] but similar to what we recently discussed for water-DME mixtures [49]. Maximal (negative) deviation from the ideal type behaviour reported from the experimental measurements is at $X_{\text{dme}} \approx 0.45$. The simulations results reproduce the position of a minimum approximately; namely the minimum is in the interval 0.3–0.4, dependent on the model employed. These trends are in concordance with our observations concerning deviations from ideality of thermodynamic properties and self-diffusion coefficients. However, the magnitude of the excess static dielectric constant is overestimated from the simulated models. The TIP4P-Ew combined with CS2 model is the most close to the experimental data. It is worth mentioning that the excess dielectric

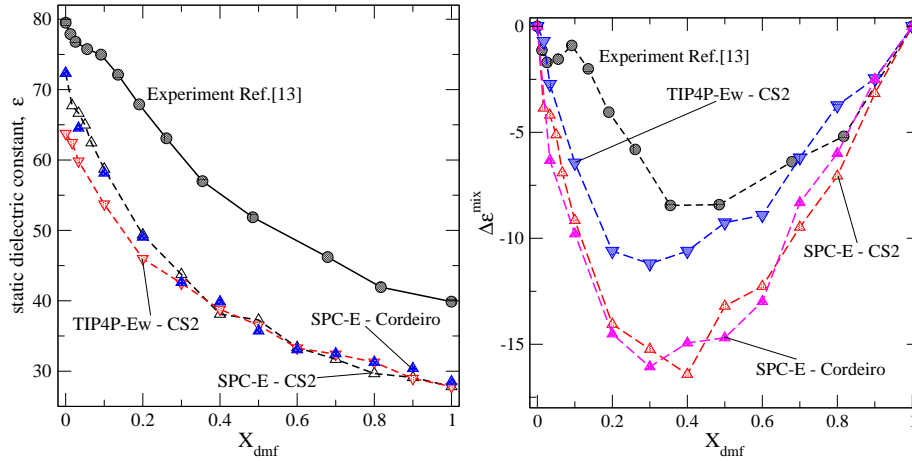


Figure 10. (Color online) Panel (a): Composition dependence of the static dielectric constant of water-DMF mixtures from constant pressure-constant temperature simulations ($T = 298.15$ K, $P = 1$ bar) in comparison with the experimental data from [13]. Panel (b): Excess mixing static dielectric constant on composition in comparison with experimental data.

constant curve as a function of chemical composition of the mixture can be related to the excess refractive index measurements, see, e.g., [15]. This issue has not been studied at the level of the united atom models for DMF so far.

All the above results have been obtained by using isobaric-isothermal simulations of water-DMF mixtures. The final configurations of particles, however, can be conveniently used to explore one of the interfacial properties by switching to the canonical, NVT , ensemble, namely the surface tension on composition.

3.5. Surface tension of water-DMF mixtures

The simulations aiming in surface tension calculations at each point of composition axis have been performed by taking the final configuration of particles from the isobaric run. Next, the box edge along z -axis was extended by a factor of 3, generating a box with liquid slab and two liquid-mixture-vacuum interfaces in the x - y plane, in close similarity to the procedure applied in [45]. The total number of particles, three thousand, is reasonable to yield an area of the x - y face of the liquid slab sufficiently big. The elongation of the liquid slab along z -axis is sufficient as well. The executable molecular dynamics file was modified by deleting a fixed pressure condition just preserving V-rescale thermostating with the same parameters as in NPT runs. Other corrections have not been employed.

The values for the surface tension, γ , follow from the combination of the time averages for the components of the pressure tensor,

$$\gamma = \frac{1}{2}L_z \left\langle \left[P_{zz} - \frac{1}{2}(P_{xx} + P_{yy}) \right] \right\rangle, \quad (4)$$

where P_{ij} ($i, j = x, y, z$) are the components of the pressure tensor, and $\langle \dots \rangle$ denotes the time average. We performed a set of runs at a constant volume, 5–6 each with the time duration of 10 ns, and obtained the result for γ by taking the block average.

As in the previous subsections, the results concern the SPC-E-CS2, SPC-E-Cordeiro and TIP4P-EW-CS2 models. It is necessary to emphasize that our calculations were not focused to precisely reproduce the values for γ at a single point corresponding to pure water at a given density, see, e.g., [60]. We rather obtain γ at a density of each mixture coming out from the NPT simulation. These values deviate from the experimental data as we have discussed in the corresponding subsection reporting the results. The experimental value of γ reported in literature for water is 71.73 mN/m whereas for DMF it is 34.4 mN/m.

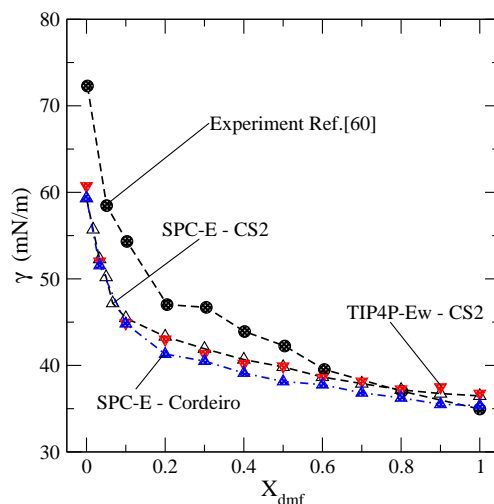


Figure 11. (Color online) Composition dependence of the surface tension of water-DMF mixtures from constant volume-constant temperature simulations ($T = 298.15$ K) in comparison with the experimental data from [61].

Our data for pure water models (SPC-E and TIP4P-Ew) agree with the data given in [60] (see table III and table IV) prior the application of the tail correction.

A set of data obtained in the present simulation work is given in figure 11, the experimental data are from the pioneering study [61]. The change of slope of the surface tension experimental curve around 30 mole percent of DMF together with the maximum of the viscosity curve at this composition (not shown here), apparently may be related to the formation of a dihydrate of DMF. Moreover, peculiarities of the mixing properties seen as a maximal deviation from an ideal type of behavior and the minimum of D_{dmf} support this assumption. We are not aware of any spectroscopy results supporting this point of view.

However, general trends of the experimental dependence of the surface tension on X_{dmf} are reproduced by the models used in simulations. The values of γ are underestimated in the water-rich mixtures. It seems that a better description of the surface tension of pure water should decrease this inaccuracy. By contrast, in the DMF-rich mixtures, the values for surface tension of mixtures are closer to the experimental data. The CS2 model for DMF satisfactorily describes the surface tension of a pure organic liquid. The Cordeiro model also yields a reasonable value of the surface tension. On the other hand, the application of TIP4P-Ew water model does not provide an improvement of the trends of behavior of γ , comparing to the SPC-E-CS2 model. Computer simulation results of this set of models do not evidence a peculiar behavior of surface tension at $X_{\text{dmf}} \approx 0.3$. We proceed now to the final comments, summary and conclusions.

4. Summary and conclusions

The mixtures explored in this work are an example of combined water-organic liquid solvents. We performed extensive molecular dynamic simulations in the isobaric-isothermal ensemble to study the density, an ample set of mixing properties and the microscopic structure of water-DMF mixtures in the entire range of solvent composition. The self-diffusion coefficients of species and the dielectric constant were calculated as well. All the simulations were performed at room temperature and ambient pressure, 1 bar. Two water models (SPC-E and TIP4P-Ew), combined with the united atom type CS2 and Cordeiro models for DMF were studied. These insights are complemented by the surface tension simulations for water-DMF mixtures using constant volume-constant temperature conditions. The values for volume were chosen from the results of the isobaric simulations.

From a comparison with the available experimental data for different properties and with the results of other authors on this and related systems, we conclude that the predictions obtained are qualitatively

correct and give a physically sound picture of the properties explored. All the properties investigated are sensitive to the composition of a water-organic liquid solvent.

The principal conclusions of the present study can be resumed as follows. We explored the evolution of the microscopic structure in terms of the pair distribution functions. The simulation results witness that the structure of the subsystem of DMF species is more inert or less sensitive to the composition, in comparison to the structure of an aqueous subsystem. The pair distribution functions evidence a heterogeneous density distribution at local scale upon adding of DMF molecules. These trends of changes of the microscopic structure bear similarity to water-DMSO and water-DME co-solvent mixtures, see, e.g., [48, 49]. Possibly the “associated” species involving water and DMF molecules can be formed in the system, with or without hydrogen bonds. This observation is in accordance with the interpretation of experimental data. Water-water and water-organic co-solvent average number of hydrogen bonds do not show a peculiar behaviour, in comparison to qualitatively similar mixtures of water with organic co-solvent [48, 49].

Dynamic properties are discussed in terms of the self-diffusion coefficients of species, D_w and D_{dmf} . Both of them exhibit a minimum in the interval of composition that corresponds to most “packed” structures according to the behaviour of a mixing volume. The values of self-diffusion coefficients of the species for pure components are reasonably well described. Concerning the dependence of the static dielectric constant on composition, we observe that its excess is better described while using the TIP4P-Ew water model combined with the CS2 model for DMF. It would be of interest to relate the behaviour of the static dielectric constant on the composition with refractive index and viscosity data. Finally, we obtained a reasonable description of the dependence of surface tension on composition, a better agreement with experimental data is expected from application of other water models.

At the present stage of the development, there are several missing elements worthwhile a detailed investigation. Namely, the application of all-atom force fields for the DMF molecules for the description of water-DMF mixtures will be reported in a separate publication. A comparison of united-atom type models with all-atom modelling is of primordial importance. On the other hand, insights into the behaviour of dynamic and dielectric properties by exploration of, e.g., the relaxation times, viscosity, hydrogen-bonds life-time and complex dielectric constant, would be desirable. Further research is planned in exploration of solutions with complex molecules in water-DMF mixtures along the lines of the available in literature experimental research.

Acknowledgements

O.P. is grateful to D. Vazquez and M. Aguilar for technical support of this work at the Institute of Chemistry of the UNAM.

References

1. Kroschwitz J.I., Seidel A. (Eds.), Kirk-Othmer Encyclopedia of Chemical Technology, Vol. 1, Wiley-Interscience, Hoboken, 2004.
2. Fiorito A., Larese F., Molinari S., Zanin T., Am. J. Ind. Med., 1997, **32**, 255, doi:10.1002/(SICI)1097-0274(199709)32:3<255::AID-AJIM11>3.0.CO;2-U.
3. Ohara M., Takagaki A., Nishimura S., Ebitani K., Appl. Catal. A, 2010, **383**, 149, doi:10.1016/j.apcata.2010.05.040.
4. Ohtaki H., Itoh S., Yamaguchi T., Ishiguro S., Rode B.M., Bull. Chem. Soc. Jpn., 1983, **56**, 3406, doi:10.1246/bcsj.56.3406.
5. Okada M., Ibuki K., Ueno M., Bull. Chem. Soc. Jpn., 2012, **85**, 189, doi:10.1246/bcsj.20110233.
6. Biliškov N., Baranović G., J. Mol. Liq., 2009, **144**, 155, doi:10.1016/j.molliq.2008.11.004.
7. Schoester P.C., Zeidler M.D., Radnai T., Bopp P.A., Z. Naturforsch. A: Phys. Sci., 1995, **50**, 38, doi:10.1515/zna-1995-0106.
8. Guarino G., Ortona O., Sartorio R., Vitagliano V., J. Chem. Eng. Data, 1985, **30**, 366, doi:10.1021/je00041a039.
9. Volpe C.D., Guarino G., Sartorio R., Vitagliano V., J. Chem. Eng. Data, 1986, **31**, 37, doi:10.1021/je00043a012.
10. Bernal-García J.M., Guzmán-López A., Cабrales-Torres A., Estrada-Baltazar A., Iglesias-Silva G.A., J. Chem. Eng. Data, 2008, **53**, 1024, doi:10.1021/je700671t.

11. De Visser C., Perron G., Desnoyers J.E., Heuvelsland W.J.M., Somsen G., *J. Chem. Eng. Data*, 1977, **22**, 74, doi:10.1021/je60072a016.
12. Cilense M., Benedetti A.V., Vollet D.R., *Thermochim. Acta*, 1983, **63**, 151, doi:10.1016/0040-6031(83)80080-X.
13. Kumbharkhane A.C., Puranik S.M., Mehrotra S.C., *J. Solution Chem.*, 1993, **22**, 219, doi:10.1007/BF00649245.
14. Checoni R.F., Volpe P.L.O., *J. Solution Chem.*, 2010, **39**, 259, doi:10.1007/s10953-010-9500-6.
15. Gofurov Sh., Ismailova O., Makhmanov U., Kokhkharov A., *Int. J. Chem. Mol. Nucl. Mater. Metall. Eng.*, 2017, **11**, 330.
16. Ueno M., Mitsui R., Iwahashi H., Tsuchihashi N., Ibuki K., *J. Phys. Conf. Ser.*, 2010, **215**, 1, doi:10.1088/1742-6596/215/1/012074.
17. Scharlin P., Steinby K., Domańska U., *J. Chem. Thermodyn.*, 2002, **34**, 927, doi:10.1006/jcht.2002.0946.
18. Han K.-J., Oh J.-H., Park S.-J., Gmehling J., *J. Chem. Eng. Data*, 2005, **50**, 1951, doi:10.1021/je050209y.
19. García B., Alcalde R., Leal J.M., Matos J.S., *J. Phys. Chem. B*, 1997, **101**, 7991, doi:10.1021/jp9626374.
20. Shokouhi M., Jalili A.H., Hosseini-Jenab M., Vahidi M., *J. Mol. Liq.*, 2013, **186**, 142, doi:10.1016/j.molliq.2013.07.005.
21. Chen L., Groß T., Lüdemann H.-D., *Z. Phys. Chem.*, 2000, **214**, 239, doi:10.1524/zpch.2000.214.2.239.
22. Jadżyn J., Świergiel J., *Phys. Chem. Chem. Phys.*, 2012, **14**, 3170, doi:10.1039/C2CP23960D.
23. Egorov G.I., Makarov D.M., Kolker A.M., *Russ. J. Phys. Chem. A*, 2007, **81**, 528, doi:10.1134/S003602440704005X.
24. Bai T.-C., Yao J., Han S.-J., *J. Chem. Thermodyn.*, 1998, **30**, 1347, doi:10.1006/jcht.1998.0402.
25. Bai T.-C., Yao J., Han S.-J., *Fluid Phase Equilib.*, 1998, **152**, 283, doi:10.1016/S0378-3812(98)00402-6.
26. Schmid E.D., Brodbek E., *J. Chem. Phys.*, 1983, **78**, 1117, doi:10.1063/1.444895.
27. Schmid E.D., Brodbek E., *J. Mol. Struct. THEOCHEM*, 1984, **108**, 17, doi:10.1016/0166-1280(84)80095-0.
28. Jorgensen W.L., Swenson C.J., *J. Am. Chem. Soc.*, 1985, **107**, 569, doi:10.1021/ja00289a008.
29. Yashonath S., Rao C.N.R., *Chem. Phys.*, 1991, **155**, 351, doi:10.1016/0301-0104(91)80111-T.
30. Cordeiro J.M.M., *Int. J. Quantum Chem.*, 1997, **65**, 709, doi:10.1002/(SICI)1097-461X(1997)65:5<709::AID-QUA37>3.0.CO;2-U.
31. Cordeiro J.M.M., Freitas L.C.G., *Z. Naturforsch. A: Phys. Sci.*, 1999, **54**, 110, doi:10.1515/zna-1999-0204.
32. Cordeiro M.A.M., Santana W.P., Cusinato R., Cordeiro J.M.M., *J. Mol. Struct. THEOCHEM*, 2006, **759**, 159, doi:10.1016/j.theochem.2005.11.016.
33. Radnai T., Bakó I., Jedlovský P., Pálinkás G., *Mol. Simul.*, 1996, **16**, 345, doi:10.1080/08927029608024084.
34. Chalaris M., Samios J., *J. Chem. Phys.*, 2000, **112**, 8581, doi:10.1063/1.481460.
35. Chalaris M., Samios J., *J. Mol. Liq.*, 1998, **78**, 201, doi:10.1016/S0167-7322(98)00092-0.
36. Chalaris M., Koufou A., Samios J., *J. Mol. Liq.*, 2002, **101**, 69, doi:10.1016/S0167-7322(02)00103-4.
37. Zoranić L., Mazighi R., Sokolić F., Perera A., *J. Phys. Chem. C*, 2007, **111**, 15586, doi:10.1021/jp0736894.
38. Zoranić L., Mazighi R., Sokolić F., Perera A., *J. Chem. Phys.*, 2009, **130**, 124315, doi:10.1063/1.3093071.
39. Gao J., Pavelites J.J., Habibollahzadeh D., *J. Phys. Chem.*, 1996, **100**, 2689, doi:10.1021/jp9521969.
40. Biswas S., Mallik B.S., *J. Chem. Eng. Data*, 2014, **59**, 3250, doi:10.1021/je5002544.
41. Vasudevan V., Mushrif S.H., *J. Mol. Liq.*, 2015, **206**, 338, doi:10.1016/j.molliq.2015.03.004.
42. Lei Y., Li H., Pan H., Han S., *J. Phys. Chem. A*, 2003, **107**, 1574, doi:10.1021/jp026638+.
43. Jia G.-Z., Huang K.-M., Yang L.-J., Yang X.-Q., *Int. J. Mol. Sci.*, 2009, **10**, 1590, doi:10.3390/ijms10041590.
44. Razzokov D., Ismailova O.B., Mamatkulov Sh.I., Trunilina O.V., Kokhkharov A.M., *Russ. J. Phys. Chem. A*, 2014, **88**, 1500, doi:10.1134/S0036024414090271.
45. Fischer N.M., van Maaren P.J., Ditz J.C., Yildirim A., van der Spoel D., *J. Chem. Theory Comput.*, 2015, **11**, 2938, doi:10.1021/acs.jctc.5b00190.
46. Galicia-Andrés E., Pusztai L., Temleitner L., Pizio O., *J. Mol. Liq.*, 2015, **209**, 586, doi:10.1016/j.molliq.2015.06.045.
47. Galicia-Andrés E., Dominguez H., Pusztai L., Pizio O., *Condens. Matter Phys.*, 2015, **18**, 43602, doi:10.5488/CMP.18.43602.
48. Gujt J., Cázares Vargas E., Pusztai L., Pizio O., *J. Mol. Liq.*, 2017, **228**, 71, doi:10.1016/j.molliq.2016.09.024.
49. Gujt J., Dominguez H., Sokolowski S., Pizio O., *Condens. Matter Phys.*, 2017, **20**, 33603, doi:10.5488/CMP.20.33603.
50. Takamuku T., Shimomura T., Tachikawa M., Kanzaki R., *Phys. Chem. Chem. Phys.*, 2011, **13**, 11222, doi:10.1039/C0CP00338G.
51. Takamuku T., Yamaguchi A., Matsuo D., Tabata M., Kumamoto M., Nishimoto J., Yoshida K., Yamaguchi T., Nagao M., Otomo T., Adachi T., *J. Phys. Chem. B*, 2001, **105**, 6236, doi:10.1021/jp003011n.
52. Takamuku T., Yamaguchi A., Matsuo D., Tabata M., Yamaguchi T., Otomo T., Adachi T., *J. Phys. Chem. B*, 2001, **105**, 10101, doi:10.1021/jp011692w.

53. Takamuku T., Noguchi Y., Yoshikawa E., Kawaguchi T., Matsugami M., Otomo T., J. Mol. Liq., 2007, **131–132**, 131, doi:10.1016/j.molliq.2006.08.048.
54. Van der Spoel D., Lindahl E., Hess B., Groenhof G., Mark A.E., Berendsen H.C., J. Comput. Chem., 2005, **26**, 1701, doi:10.1002/jcc.20291.
55. Berendsen H.J.C., Grigera J.R., Straatsma T.P., J. Phys. Chem., 1987, **91**, 6269, doi:10.1021/j100308a038.
56. Horn H.W., Swope W.C., Pitera J.W., Madura J.D., Dick T.J., Hura G.L., Head-Gordon T., J. Chem. Phys., 2004, **120**, 9665, doi:10.1063/1.1683075.
57. Vega C., Abascal J.L.F., Phys. Chem. Chem. Phys., 2011, **13**, 19663, doi:10.1039/C1CP22168J.
58. Wensink E.J.W., Hoffmann A.C., van Maaren P.J., van der Spoel D., J. Chem. Phys., 2003, **119**, 7308, doi:10.1063/1.1607918.
59. Alejandro J., Chapela G.A., Saint-Martin H., Mendoza H., Phys. Chem. Chem. Phys., 2011, **13**, 19728, doi:10.1039/C1CP20858F.
60. Vega C., de Miguel E., J. Chem. Phys., 2007, **126**, 154707, doi:10.1063/1.2715577.
61. Blankenship F., Clampitt B., Proc. Oklahoma Acad. Sci., 1950, **31**, 106.

Залежність від концентрації мікроскопічної структури, термодинамічних, динамічних та електричних властивостей модельної суміші вода-диметил формамід. Результати симуляцій методом молекулярної динаміки

Г. Домінгес, О. Пізіо

Інститут матеріалознавства, Національний автономний університет м. Мехіко, Мехіко, Мексика

Здійснено симуляції методом молекулярної динаміки в ізотермічно-ізобаричному ансамблі з метою вивчення широкого набору властивостей моделі суміші вода-N,N-диметилформамід (DMF) як функцій концентрації. Використано моделі води SPC-E і TIP4P-Ew разом з двома об'єднаними атомними моделями для DMF [Chalaris M., Samios J., J. Chem. Phys., 2000, **112**, 8581; Cordeiro J., Int. J. Quantum Chem., 1997, **65**, 709]. Наш основний аналіз стосується поведінки структурних властивостей в термінах радіальних функцій розподілу і числа водневих зв'язків між молекулами різних сортів, а також термодинамічних властивостей. Зокрема, ми досліджуємо густину, надлишкові молярний об'єм та ентальпію змішування, питому теплоємність і надлишкову питому теплоємність змішування. Накінець, обговорюються коефіцієнти самодифузії сортів і діелектрична стала системи. Крім того, обчислюється та аналізується поверхневий натяг сумішей вода-DMF.

Ключові слова: моделі води, моделі N,N-диметилформаміду, термодинамічні властивості, коефіцієнт самодифузії, діелектрична стала, поверхневий натяг, молекулярна динаміка
